Stem Cell Reports
Resource
ISSCR
OPEN ACCESS

Development of a platform to investigate long-term potentiation in human iPSC-derived neuronal networks

Deborah Pré,[1] Alexander T. Wooten,[1] Steven Biesmans,[1,3] Sandy Hinckley,[1,4] Haowen Zhou,[1] Sean P. Sherman,[1,5] Priyanka Kakad,[1,6] Jeffrey Gearhart,[2] and Anne G. Bang[1,*]

[1]Conrad Prebys Center for Chemical Genomics, Sanford Burnham Prebys Medical Discovery Institute, 10901 North Torrey Pines Road, La Jolla, CA 92037, USA

[2]Henry M. Jackson Foundation for the Advancement of Military Medicine on Contract to USAF School of Aerospace Medicine, Wright-Patterson AFB, Dayton, OH 45433, USA

[3]Present address: UCB Ventures, Allée de la Recherche 60, 1070 Brussels, Belgium

[4]Present address: QurAlis, 100 Cambridgepark Drive, Suite 500, Cambridge, MA 02140, USA

[5]Present address: Fate Therapeutics, Inc., 12278 Scripps Summit Dr., San Diego, CA 92131, USA

[6]Present address: iXCells Biotechnologies, 7270 Trade St., San Diego, CA 92121, USA

*Correspondence: abang@sbpdiscovery.org

https://doi.org/10.1016/j.stemcr.2022.07.012

SUMMARY

Impairment of long-term potentiation (LTP) is a common feature of many pre-clinical models of neurological disorders; however, studies in humans are limited by the inaccessibility of the brain. Human induced pluripotent stem cells (hiPSCs) provide a unique opportunity to study LTP in disease-specific genetic backgrounds. Here we describe a multi-electrode array (MEA)-based assay to investigate chemically induced LTP (cLTP) across entire networks of hiPSC-derived midbrain dopaminergic (DA) and cortical neuronal populations that lasts for days, allowing studies of the late phases of LTP and enabling detection of associated molecular changes. We show that cLTP on midbrain DA neuronal networks is largely independent of the N-methyl-D-aspartate receptor (NMDAR) and partially dependent on brain-derived neurotrophic factor (BDNF). Finally, we describe activity-regulated gene expression induced by cLTP. This cLTP-MEA assay platform will enable phenotype discovery and higher-throughput analyses of synaptic plasticity on hiPSC-derived neurons.

INTRODUCTION

The advent of human induced pluripotent stem cell (hiPSC) technology (Nakagawa et al., 2008; Takahashi et al., 2007) has provided unique opportunities to study neurological disorders because of the difficulties accessing the human brain. Although animal models have been crucial for studies of neurological disease (Kolb, 1984), they are limited because they do not reflect aspects of development, genetics, and disease mechanisms unique to the human brain. These experimental gaps can potentially be addressed by hiPSCs. Indeed, there has been a great deal of progress in the development of methods to produce brain cells from hiPSCs (Hasselmann and Blurton-Jones, 2020; Tao and Zhang, 2016), positioning the field to develop *in vitro* constructs that reflect the functionality of the human brain.

A crucial aspect of neuronal function is the ability to modify the strength and efficacy of synaptic transmission through activity-dependent mechanisms, collectively referred to as synaptic plasticity. Synaptic plasticity is critical across many processes, including development, homeostasis, learning and memory, and recovery from injury (Mateos-Aparicio and Rodriguez-Moreno, 2019). The most widely studied form of synaptic plasticity is long-term potentiation (LTP), which leads to long-lasting strengthening of synapses in response to specific types of stimulation (Bliss and Lomo, 1973; Nicoll, 2017). LTP is considered the biological substrate for learning and memory, and its impairment is a prominent feature of many pre-clinical models of neurological disorders, including Alzheimer's disease (Selkoe, 2002), Parkinson's disease (Picconi et al., 2012), autism (Jung et al., 2013), schizophrenia (Mould et al., 2021), bipolar disorder (Zak et al., 2018), and drug addiction (Mameli and Luscher, 2011). Thus, establishing approaches to assess LTP in hiPSC-derived neurons is essential for disease modeling.

Extensive research over the last decades has focused on different forms of LTP, including postsynaptic and presynaptic forms, those that depend on the N-methyl-D-aspartate receptor (NMDAR) subclass of glutamate receptors (Luscher and Malenka, 2012), and those that are NMDAR independent (Alkadhi, 2021). Regardless of the form of LTP, at nearly all glutamatergic synapses, LTP induction depends on an initial rise in cytosolic Ca^{2+} concentration via NMDARs, voltage-gated calcium channels (VGCCs), calcium-permeable α-amino-3-hydroxy-5-methyl-4-isoxazole propionic acid receptors (CP-AMPARs), or release from internal stores, which triggers activation of kinase cascades, including cyclic adenosine monophosphate (cAMP)-dependent protein kinase A (PKA) and Ca^{2+}/calmodulin-dependent protein kinase II (CaMKII), that potentiate synaptic transmission (Nicoll, 2017; Padamsey et al., 2019). These initial events, known as early-phase

LTP (E-LTP), rely on protein trafficking, whereas, during the subsequent late phase of LTP (L-LTP), longer-lasting changes are elicited in a transcription-dependent manner, leading to stabilization of synaptic enlargement (Baltaci et al., 2019). Other factors also contribute to the induction and maintenance of LTP. For example, the receptor tyrosine kinase TrkB, activated by its ligand brain-derived neurotrophic factor (BDNF), is a potent modulator of multiple forms of LTP (Johnstone and Mobley, 2020).

LTP is typically induced through high-frequency tetanic stimulation of the presynaptic axon of a synapse (Nicoll, 2017), which has the drawback of transiently activating only a small number of synapses. To overcome this limitation, chemical stimulation protocols have been developed to induce LTP across many synapses, enabling studies of network-wide effects and increasing the feasibility of detecting associated molecular changes (Molnar, 2011). Here we take advantage of this approach to develop a platform to study LTP in networks of hiPSC-derived neurons, using a chemical LTP (cLTP) protocol based on the adenylate cyclase activator forskolin (FSK) and the phosphodiesterase inhibitor rolipram (ROL) to increase cAMP levels, activating PKA and stimulating the biochemical machinery that underlies LTP (Otmakhov et al., 2004). We developed the assay on multi-electrode arrays (MEAs), which allow recording across a neuronal network in a non-invasive manner over extended periods of time that are critical for L-LTP. MEAs have been broadly used to study synaptic plasticity (Brofiga et al., 2021), including with chemical paradigms on rodent neurons (Arnold et al., 2005; Niedringhaus et al., 2012; Pegoraro et al., 2010).

Here, to study LTP on hiPSC-derived neuronal networks, we applied FSK/ROL-mediated cLTP to hiPSC-derived midbrain-dopaminergic and cortical neuronal populations on 48-well MEA plates that facilitate higher throughput analyses. Like cultures of primary rodent neurons (Opitz et al., 2002), hiPSCs and human embryonic stem cell-derived neurons self-organize into networks that generate spontaneous, synchronous bursts of action potentials across electrodes, termed network bursts (NBs) (Heikkila et al., 2009; Odawara et al., 2014). We demonstrate that FSK/ROL-mediated cLTP induces long-lasting increases in firing rate and NB frequency up to 72 h after drug washout. We show that these effects on midbrain-dopaminergic neuronal networks are largely independent of the NMDAR; independent of L-, R- and T-type VGCCs and CP-AMPAR; and partially dependent on BDNF and other unidentified factors released into the medium. Finally, we demonstrate that, in response to FSK/ROL treatment, there is a rapid increase in phosphorylated cAMP-response element-binding protein (CREB) and induction of activity-regulated gene expression. These results support the utility of this platform for investigations of LTP in hiPSC-derived neurons.

RESULTS

Characterization of the iDopa cell population

To develop an hiPSC-based assay to study LTP, we focused on commercially available hiPSC-derived dopaminergic (DA) neurons in co-culture with hiPSC-derived astrocytes (iDopa and iAstro; Fujifilm Cellular Dynamics), as consistent, cryo-preserved cell populations. Our characterization of two independent experiments by immunofluorescence and RNA sequencing (RNA-seq) of iDopa/iAstro co-cultures at a ratio of 8:1 (hereafter referred to as iDopa cultures) indicated that iDopa neurons are a mixed population of primarily midbrain DA neurons, in addition to glutamatergic and gamma-aminobutyric acid (GABA)ergic neurons, resembling cell types present across midbrain DA regions (Asgrimsdottir and Arenas, 2020; Kim et al., 2019; Poulin et al., 2020; Tiklova et al., 2019; Figures S1A–S1D). We detected expression of multiple markers described as enriched in the ventral tegmental area (VTA) or substantia nigra, suggesting that the iDopa cell population contains both types (Figure S1E). LTP is known to be important in midbrain DA nuclei, especially the VTA, where glutamatergic and GABAergic synaptic transmission are critical regulators of DA neuron activity and are thought to play important roles in neurological disease, including drug addiction and schizophrenia (Chen et al., 2021; Langlois and Nugent, 2017). Thus, there is a need to develop hiPSC-based functional assays to model LTP in the VTA.

cLTP induces long-lasting potentiation of iDopa neuronal network activity

We next assessed iDopa network activity on 48-well MEA plates (Axion BioSystems), a format that allows pharmacological interrogation of multiple independent networks. By 3–4 weeks after plating, iDopa cultures exhibited consistent baseline network activity (Table S1), as reported by others (Ronchi et al., 2021; Yokoi et al., 2019). To assess network excitation and inhibition, we treated the culture with the NMDAR blocker (2R)-amino-5-phosphonovaleric acid (APV), the AMPAR and kainate receptor blocker cyanquixaline (CNQX), and the GABA type A receptor (GABAAR) blocker picrotoxin (PTX). Results from this analysis showed that NBs were lost in the presence of CNQX (Figures S2B and S2E), strongly reduced in frequency by AP5 (Figures S2C and S2E), and increased in frequency by PTX (Figures S2D and S2E). These results suggest that, although NBs are primarily driven by and dependent on AMPARs, NMDARs also contribute to this excitatory drive, which is weakly refined by GABAAR-mediated inhibition.

We next tested an FSK/ROL-mediated cLTP paradigm (Figures 1A–1C). On the day of the assay, the medium was changed, and after 2 h, 50 μM FSK and 0.1 μM ROL were added. After 30 min, multiple medium changes were

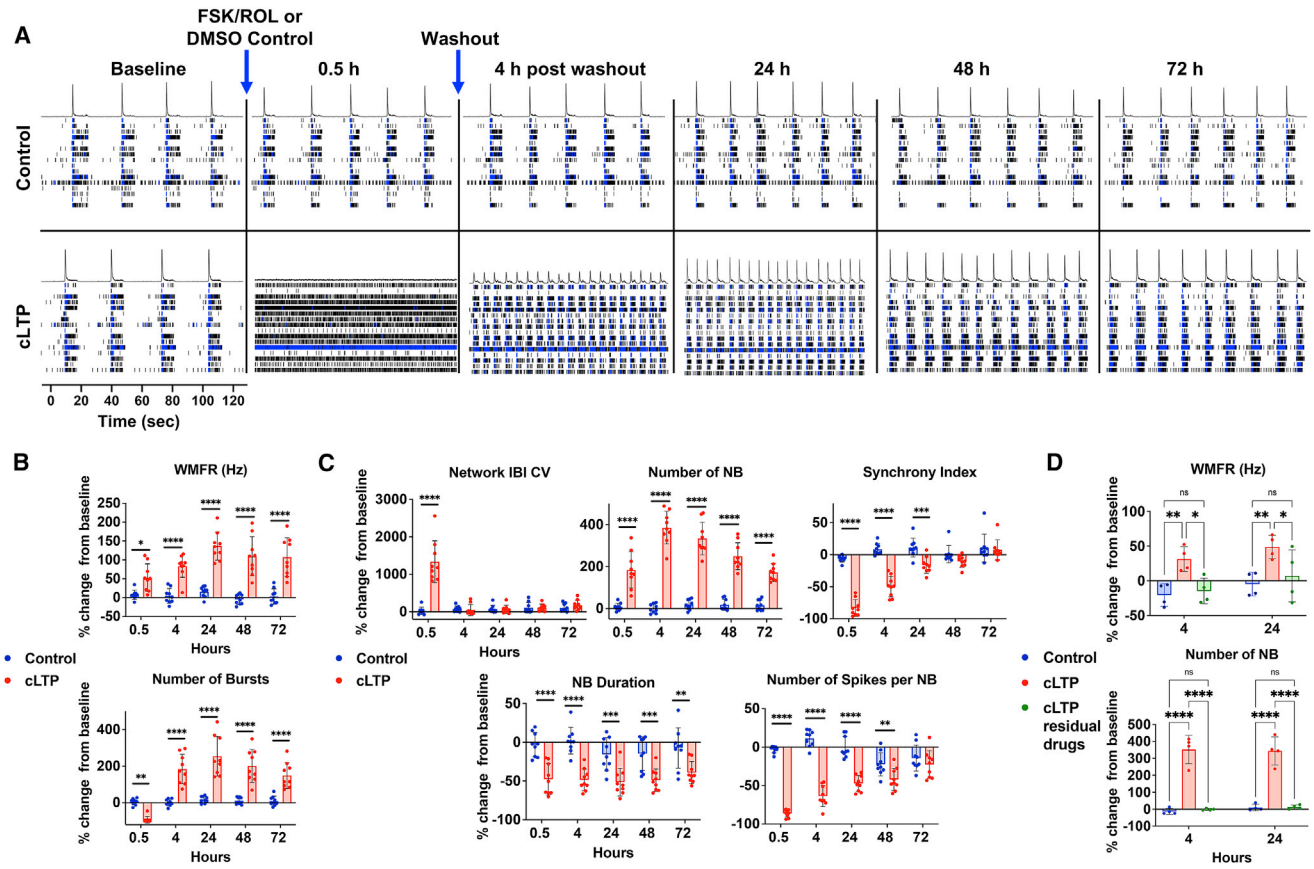

Figure 1. FSK/ROL treatment of iDopa neuronal networks potentiates activity that persists after drug washout

(A) Representative raster plots of MEA recordings from CTRL (DMSO) and cLTP-treated wells from recordings at baseline, at 30 min (while drugs are still present in the medium), and at the indicated times after FSK/ROL washout. Each row of the raster plot shows a recording from a single electrode (of 16 total electrodes), with bursts shown in blue. The histogram at the top of the raster plot shows the sum of well-wide spikes at the indicated time in seconds.

(B and C) Analysis of WMFR and bursting parameters (B) and NB and SI parameters (C) for the experiment in (A).

(D) Analysis after treatment with cLTP drugs at concentrations that model residual drugs remaining after washout (FSK = 41.6 nM, ROL = 83.3 pM) versus those used to elicit cLTP (FSK = 50 μM, ROL = 0.1 μM).

Wells per treatment group: (B) and (C), n = 9; (D), n = 4. two-way ANOVA, Sidak's multiple comparison test. Data are shown as mean ± SD, and p values are indicated as *0.05 > p ≥ 0.01; **0.01 > p ≥ 0.001; ***0.001 > p ≥ 0.0001; ****p < 0.0001. The experiment is representative of more than 10 independent experiments. See also Figure S3.

performed to wash out the drugs. Initially, during treatment with FSK/ROL, we observed disrupted network organization with increased tonic activity, as reflected by decreased numbers of bursts, increased weighted mean firing rate (WMFR; mean firing rate based on only active electrodes with activity > 5 spikes per minute), decreased network synchrony index (SI), and highly increased network inter-burst interval coefficient of variation (IBI CV), indicating that NBs are spurious and do not occur in a rhythmic pattern. By 1 h after drug washout, we observed a persistent increase in WMFR, accompanied by recovery of network organization, as indicated by return of network IBI CV to baseline levels, and an increased number of NBs that persisted for 72 h. The increased NB frequency is associated with reduced NB duration and fewer spikes per NB (Figures 1B and 1C). This observation is consistent with reports of an inverse correlation between burst frequency and burst duration, explained by a dependency on the availability of glutamate synaptic vesicles when there is a short recovery window (<30 s) after bursting (Cohen and Segal, 2011). Although, 4 h after washout, the SI is still reduced compared with baseline, it nears baseline levels by 24 h and is restored to baseline levels by 48 h (Figure 1C). By 96 h, firing and network bursting rates return to baseline levels (data not shown). In Figure 2, results from this experiment are shown as raw values to illustrate that all wells

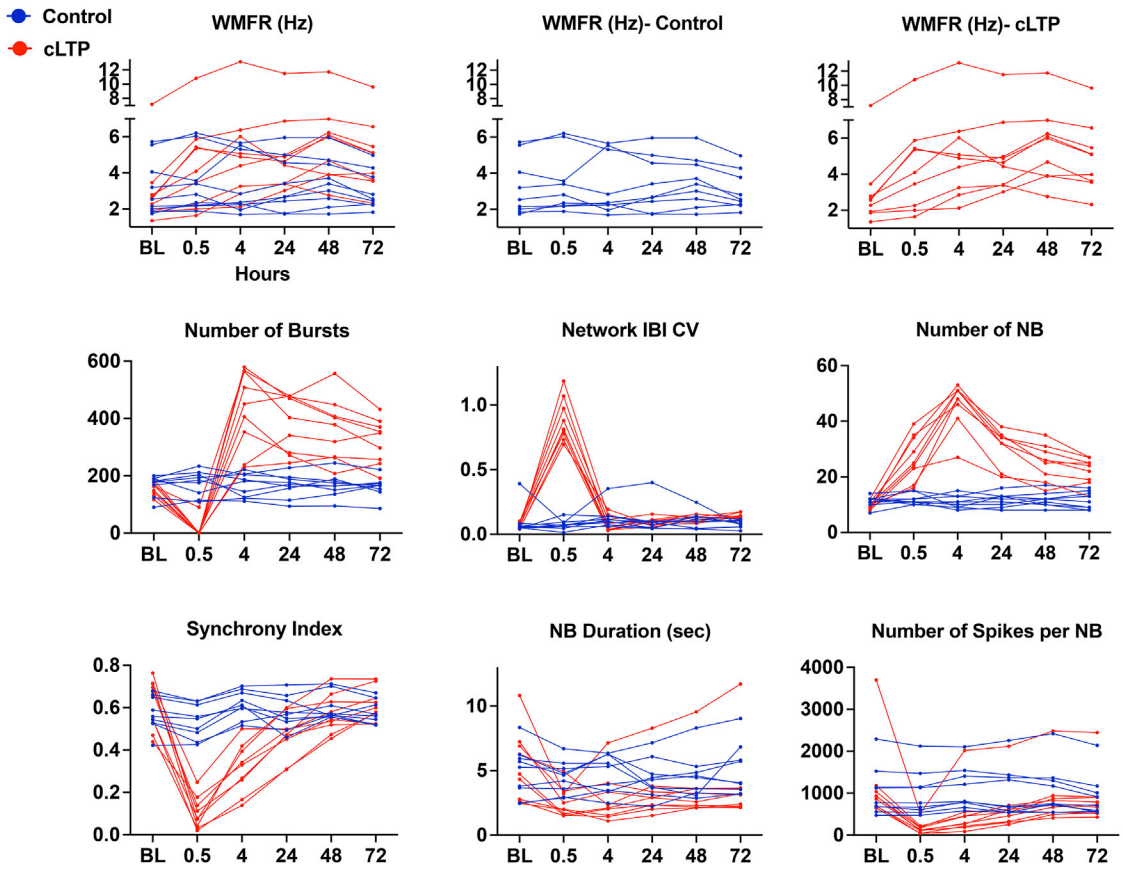

Figure 2. cLTP-treated wells respond similarly across multiple metrics relative to baseline values

Panels show the change over time for raw values for each control (blue) and FSK/ROL treated well (red) shown in Figures 1A–1C for the indicated metrics. Recordings were acquired for 5 min for each time point. For WMFR, FSK/ROL-treated and CTRL wells are graphed together as well as separately for clarity. n = 9 wells.

exhibit FSK/ROL-mediated potentiation of firing and bursting and respond similarly across multiple metrics relative to baseline values. Finally, to address the possibility that persistent increases in activity are caused by residual levels of FSK/ROL remaining after washout (approximately 42 nM and 83 pM, respectively), we show that continuous exposure to these low levels of cLTP drugs does not affect network activity (Figure 1D).

The cLTP-mediated effects were highly reproducible across eight experiments, resulting in a signature of increased WMFR and NB frequency along with decreased NB duration and spikes per NB, shown in heatmaps of significance and *Z* score for percent change from baseline for selected metrics over 72 h after drug wash-off (Figures S3A–S3C) and in raster plots (Figure S3D). Six of the eight experiments were tracked for 96 h, and four of these still exhibited the increased WMFR and NB frequency phenotype at 72 h (experiments 1–6; Figures S3A–S3C). By 96 h, network activity had returned to baseline (data not shown). These results are consistent with the interpretation that a 30-min exposure to FSK/ROL increases excitation in the network after drug washout, resulting in increased firing rates and network bursting, reflecting E-LTP initially and then L-LTP for up to 72 h.

cLTP-mediated potentiation of iDopa neuronal networks is not prevented by blocking NMDAR, CP-AMPAR, and L-, R-, and T-type VGCCs

Studies of FSK/ROL-mediated cLTP on rat hippocampal slices have led to opposite conclusions regarding NMDAR dependence. In one report, cLTP was shown to be NMDAR independent under adenosine A1 receptor blockade (Lu and Gean, 1999), but in another, cLTP was blocked by APV (Otmakhov et al., 2004). Recent studies of FSK/ROL-induced plasticity on hiPSC-derived cortical neurons also reported NMDAR dependence (Fink et al., 2021). Thus, we investigated the effects of blocking NMDAR with APV on FSK/ROL-mediated cLTP. iDopa cultures were pretreated with 50 μM APV for 30 min, eliciting the expected decrease in NB frequency (Figures 3A and 3B).

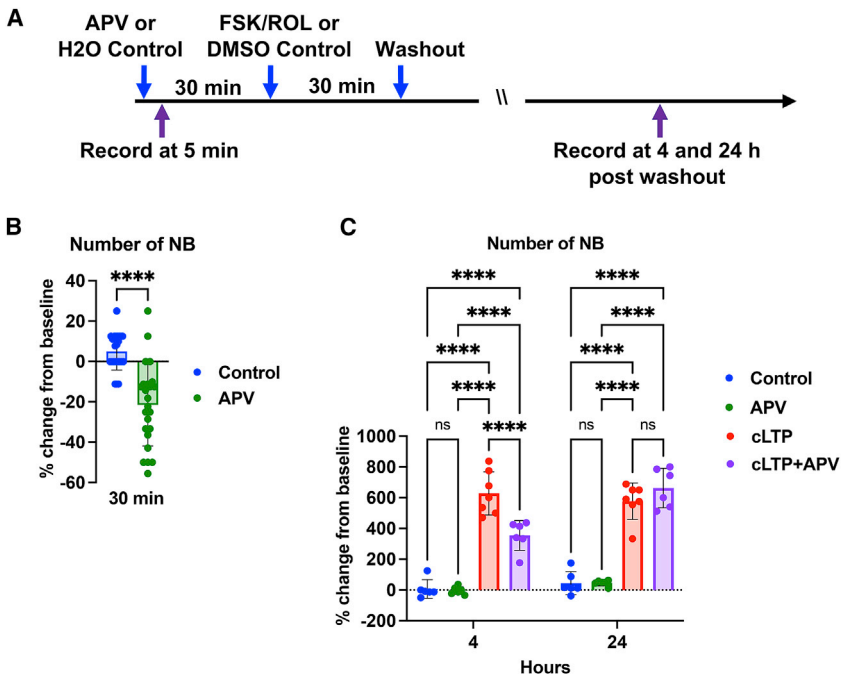

Figure 3. FSK/ROL-mediated cLTP on iDopa neuronal networks is largely NMDAR-independent

(A) Timeline of drug additions/washouts and recording time points.

(B) Analysis of response to APV pretreatment. n = 24 wells per treatment group. Unpaired t test.

(C) Analysis of cLTP on APV-treated wells. n = 6 wells per treatment group.

Two-way ANOVA, Tukey's multiple comparisons test. Data are shown as mean ± SD, and p values are indicated as *0.05 > p ≥ 0.01; **0.01 > p ≥ 0.001; ***0.001 > p ≥ 0.0001; ****p < 0.0001. The experiment is representative of three independent experiments.

After APV pretreatment, FSK/ROL were added for 30 min, followed by APV/FSK/ROL washout (Figure 3A). We observed that, for control wells treated with APV, NB frequency returned to baseline after drug washout (Figure 3C). However, for cLTP wells treated with APV, we observed a mild reduction in NB frequency 4 h after FSK/ROL/APV washout but not at 24 h (Figure 3C). This suggests that although there is a minor contribution, cLTP is largely NMDAR independent. We then considered dependence on two other potential sources of calcium entry associated with some forms of NMDAR-independent LTP: L-type VGCCs and CP-AMPARs (Alkadhi, 2021). Using a similar paradigm as described above (pretreatment, followed by addition of FSK/ROL and then drug washout), we tested the L-type VGCC blocker nifedipine (100 μM) and the CP-AMPAR blocker 1-naphthyl acetyl spermine (NASPM) (4.8 μM). We observed that neither reduced cLTP-induced potentiation (Figures S4A and S4B) and that nifedipine caused a mild increase in NB frequency, as reported previously for rat hippocampal neurons on MEAs (Arnold et al., 2005). Finally, because FSK-induced plasticity is thought to have a presynaptic component (Chavez-Noriega and Stevens, 1994; Kaneko and Takahashi, 2004; Sakaba and Neher, 2001), we considered the contribution of R-type VGCCs, a source of calcium entry associated with some presynaptic forms of LTP (Castillo, 2012). As we observed for nifedipine and NASPM, $NiCl_2$ (500 μM), which selectively blocks R- and T-type VGCCs, did not decrease cLTP-induced potentiation; however, it did cause an increase in WMFR at 24 h compared with FSK/ROL alone (Figure S4C). In follow-up studies, it will be important to determine whether calcium entry is required for cLTP on iDopa neuronal networks and, if so, the source(s).

Factors released into the medium, including BDNF, contribute to the maintenance of cLTP-mediated potentiation of iDopa neuronal networks after FSK/ROL washout

BDNF is a regulator of L-LTP (Panja and Bramham, 2014; Park and Poo, 2013). Based on reported observations that cAMP elevation through FSK-induced potentiation activates TrkB and is attenuated by BDNF elimination (Patterson et al., 2001), we next explored the contribution of BDNF and TrkB to the maintenance of cLTP-mediated potentiation on iDopa cultures. First, we wanted to determine whether FSK/ROL elicited BDNF secretion. In two experiments, we observed that conditioned medium (CM) from cLTP-treated wells (cLTP-CM), collected 1 h after FSK/ROL washout, exhibited an average of 3.82 ± 0.8-fold increase in BDNF (1.44 ± 0.35 ng/mL) compared with CM from controls (CTRL-CM) (0.37 ± 0.014 ng/mL), based on an enzyme-linked immunosorbent assay (ELISA) (Figure S5). We found that, for FSK/ROL-treated wells where the medium had been removed 1 h after washout and replaced with fresh medium or CTRL-CM from vehicle-treated wells, potentiation was strongly reduced, with decreased WMFR and NB frequency 4 and 24 h after

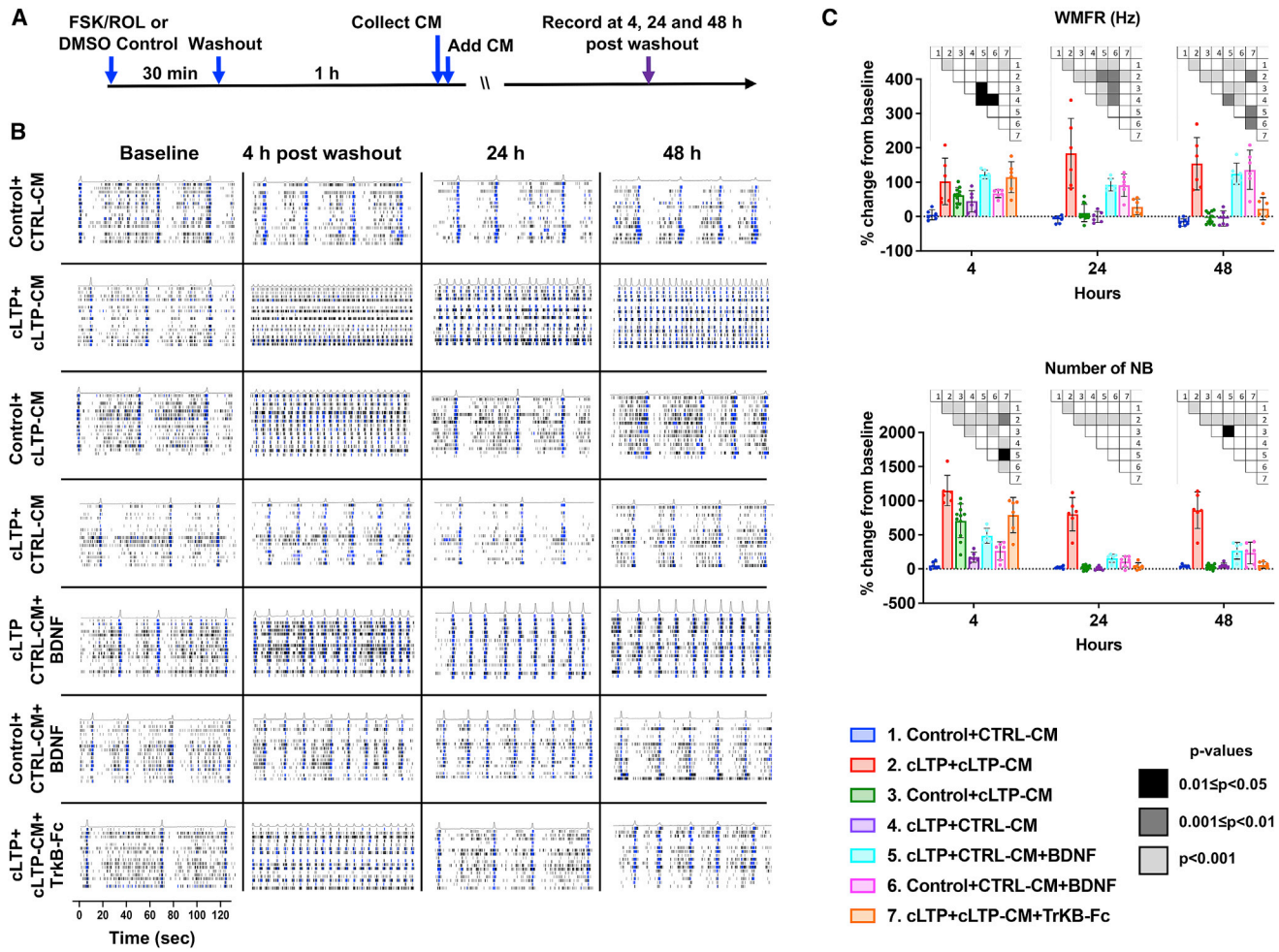

Figure 4. Factors released into the medium, including BDNF, contribute to the maintenance of cLTP-mediated potentiation of iDopa neuronal networks after FSK/ROL washout

(A) Timeline of drug and CM addition/removal and recording time points.

(B) Representative raster plots for the indicated treatments where, 1 h after FSK/ROL or vehicle washout, the medium was removed and replaced with CTRL-CM or cLTP-CM. In some wells, 8 nM BDNF or 2 mg/mL TrkB-Fc was added along with the CM. CTRL, vehicle (DMSO)-treated well; cLTP, cLTP-treated well; cLTP-CM, CM from a cLTP-treated well collected 1 h after FSK/ROL washout; CTRL-CM, CM collected 1 h after vehicle (DMSO) washout.

(C) Analysis of WMFR and number of NB parameters for the experiment shown in (A). n = 6 wells per treatment group. Two-way ANOVA, Sidak's multiple comparisons test. Data are shown as mean ± SD. The p values for crosswise comparisons are shown in boxes over graphs. The experiment is representative of three independent experiments. See also Figure S6.

FSK/ROL washout. In contrast, potentiation could be maintained when the medium was replaced with cLTP-CM (Figure S6A). Across four independent experiments, we observed that replacing medium in CTRL, vehicle-treated wells with cLTP-CM resulted in increased NB frequency at the 4-h time point. In two of the four experiments, increased NB frequency persisted until 24 h, and in one, increased WMFR was also observed at 4 h (Figure 4; data not shown). However, in contrast to FSK/ROL treatment, when cLTP-CM was added to naive CTRL wells and then washed out after 30 min, activity rapidly returned to baseline (Figure S6B). These results demonstrate that, during the first hour after FSK/ROL washout, factors necessary for cLTP maintenance are released into the medium. Our observations that addition of cLTP-CM to vehicle-treated wells induces transient potentiation whereas addition of cLTP-CM to cLTP-treated wells had longer-lasting effects suggest that the early phase of cLTP induced upon FSK/ROL addition and a late phase after drug washout are required to elicit longer-lasting potentiation.

We next tested whether cLTP-CM-mediated potentiation is BDNF dependent. First, we tested whether BDNF is

sufficient to rescue the inability of CTRL-CM to maintain potentiation after cLTP-CM has been removed from FSK/ROL-treated wells. The medium was removed 1 h after FSK/ROL or vehicle washout and replaced with CTRL-CM, to which we added 8 nM BDNF. Consistent with reports that BDNF potentiates neuronal activity (Panja and Bramham, 2014; Park and Poo, 2013), we observed that addition of CTRL-CM + BDNF to vehicle-treated wells or cLTP-treated wells resulted in increased WMFR and NB frequency at 4 h and increased WMFR, but not increased NBs, at 24 h (Figure 4). Thus, addition of BDNF was not sufficient to rescue the inability of CTRL-CM to maintain increased NB frequency at 24 h in cLTP-treated cultures. For WMFR, because CTRL-CM + BDNF caused an increase at 24 h for vehicle- and cLTP-treated wells, we could not distinguish specifically whether BDNF was sufficient to rescue the inability of CTRL-CM to maintain WMFR. We next wanted to determine whether BDNF was necessary for cLTP-CM-mediated potentiation. To block BDNF, we used a TrkB-Fc receptor body, a BDNF scavenger (Panja and Bramham, 2014). We tested cLTP-treated wells by removing the medium 1 h after FSK/ROL washout and replacing it with cLTP-CM, to which we added 2 μg/mL TrkB-Fc. In two independent experiments, addition of TrkB-Fc, but not the human immunoglobulin G (IgG) used as a CTRL, resulted in reduced WMFR and NB frequency at 24 and 48 h compared with cLTP alone (Figures 4 and S6C). Our observation that TrkB-Fc reduces but does not block cLTP-mediated potentiation suggests that BDNF is necessary to consolidate potentiation, but it is not sufficient. These experiments show that BDNF is a critical component of cLTP-CM, but other unidentified factors released into the medium are also required.

Withdrawal of stimulatory factors from the culture medium is important for FSK/ROL-mediated potentiation of iDopa neuronal networks

All cLTP experiments were conducted after withdrawal of BrainPhys supplements, which include 1 mM cAMP and 20 ng/mL BDNF (Experimental procedures). Because of the central roles of cAMP and BDNF in LTP, we wanted to determine whether it was important that these factors are withdrawn before cLTP is performed. Thus, on the day before the assay, when BrainPhys supplements are withdrawn, cAMP or BDNF was added back for the remainder of the assay. We observed that addition of 20 ng/mL BDNF does not prevent FSK/ROL-mediated potentiation; however, it does reduce the increase in number of NBs (Figure S7). In contrast, apart from a mild increase in WMFR at 4 h, potentiation is blocked when 1 mM cAMP is added (Figure S7). This result is consistent with observations that prolonged synaptic stimulation prevents LTP responses, a phenomenon known as "LTP occlusion" (Huang and Kandel, 1998), and suggests that it is important to perform the cLTP assay under conditions where stimulatory medium supplements, such as cAMP, are removed.

cLTP on iDopa neuronal networks induces phosphorylation of CREB and increased IEG protein expression

We then investigated activation of the transcription factor CREB, a major transcriptional effector of LTP (Bourtchuladze et al., 1994), by assessing phosphorylation at the PKA-dependent phosphorylation site Ser-133 in cLTP-treated iDopa cultures. As expected, in response to increased cAMP levels from FSK/ROL treatment, the number of phosphorylated CREB (phCREB)-positive neuronal nuclei increased 30 min after FSK/ROL washout and then gradually declined (Figures 5A, 5B, and 5G), suggesting immediate phosphorylation followed by progressive dephosphorylation. Consistent with CREB activation, we also observed increased protein expression of the CREB-dependent immediate-early genes (IEGs) EGR1, and FOS (Davis et al., 2003; Knapska and Kaczmarek, 2004) (Figures 5C–5F, 5H, and 5I).

cLTP on iDopa neuronal networks induces activity-regulated gene expression

The late phase of LTP relies on transcription of a canonical gene network (Bliim et al., 2016). To characterize gene expression changes induced by cLTP on iDopa cultures, we performed RNA-seq 5 h after FSK/ROL or vehicle washout on three replicates and observed 407 upregulated and 143 downregulated differentially expressed genes (DEGs) ($p < 0.05$, Benjamini-Hochberg [BH] adjusted) (Figures 6A and 6B; Table S2). Gene Ontology (GO) analysis of upregulated DEGs showed significant associations with biological process terms related to activity-regulated gene expression, such as "synaptic plasticity," "circadian rhythm" (Bolsius et al., 2021), and "glucocorticoid stimulus" (Arango-Lievano et al., 2019; Figure 6D; Table S3).

Canonical neuronal activity-regulated gene expression signatures have been described that are common across different stimulation paradigms and brain regions (Gray and Spiegel, 2019). To distinguish canonical activity-regulated gene expression, we compared upregulated DEGs induced by cLTP on iDopa cultures with two reported studies of activity-regulated gene expression in cultured neurons: (1) mouse cortical neurons induced by continuous exposure to potassium chloride (KCl), assayed at the 1- and 6-h time points (Spiegel et al., 2014), and (2) hiPSC-derived cortical neurons induced by continuous exposure to the voltage-gated potassium channel antagonist 4-aminopyridine (4AP) and the GABAAR antagonist

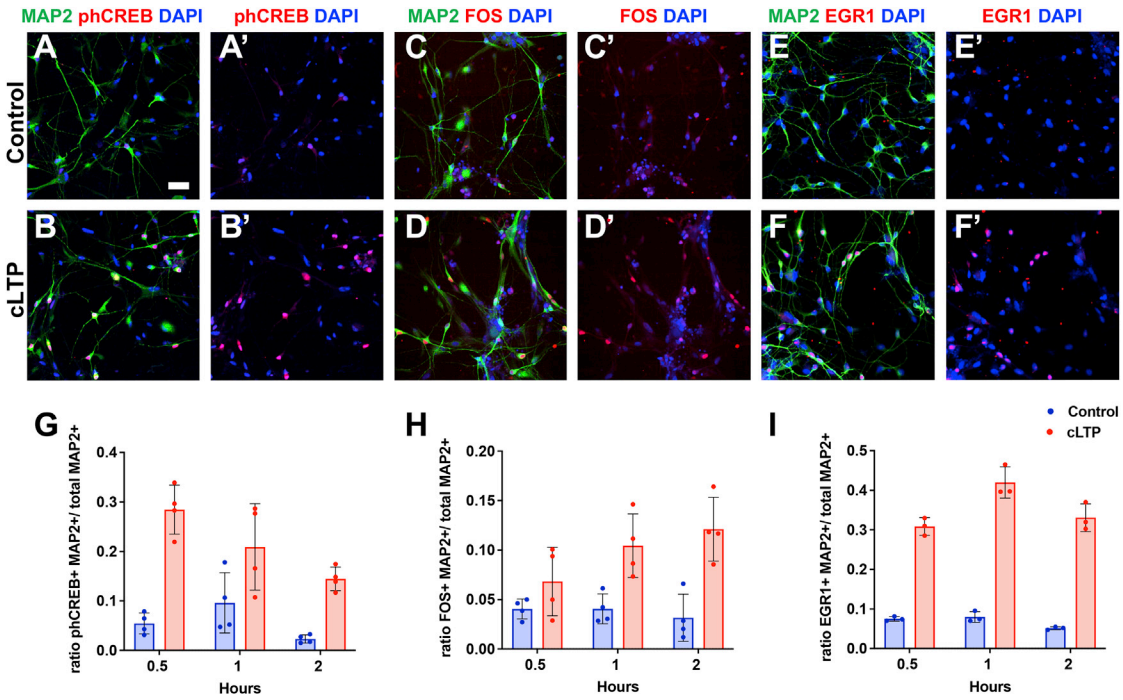

Figure 5. cLTP on iDopa neuronal networks induces phosphorylation of CREB and increased IEG protein expression

(A–F) Representative confocal images of cLTP and CTRL (DMSO)-treated cultures, fixed 30 min after FSK/ROL washout.

(A′–F′) Channels uncoupled from merges shown in (A)–(F). Cultures were immunostained with the neuronal marker MAP2 (green), the nuclear marker DAPI (blue), and, for (A) and (B), Ser 133 phCREB (red); (C) and (D), FOS (red); and (E) and (F) EGR1 (red). Scale bar in (A), 50 μm for all images shown.

(G–I) Quantification of $MAP2^+$ neurons co-positive for (G) phCREB, (H) FOS, or (I) EGR1. n = 4 wells per treatment group, 25 fields per well. Data are shown as mean ± SD.

The experiment is representative of two independent experiments.

bicuculline (BIC) at the 1- and 4-h time points (Pruunsild et al., 2017; Figure 6E; Table S4). At the 1-h time point for these two datasets, we observed 27 of 407 upregulated DE-Gs in common with the iDopa dataset, consisting primarily of transcriptional regulators (14 of 27), including IEGs whose expression presumably persisted in the cLTP-induced iDopa cultures to the 5-h time point, when RNA-seq was performed. Interestingly, three genes, reported as activity-regulated human-specific IEGs without mouse orthologs (Pruunsild et al., 2017) (*BRE-AS1*, *LINC00473*, and *ZNF331*) were also upregulated by cLTP on iDopa cultures (Table S4), underscoring the system's utility for studying the proposed evolutionary divergence of synaptic plasticity in humans and rodents (Hardingham et al., 2018; Qiu et al., 2016). Comparison of the later time points, 6 and 4 h for the mouse and hiPSC cortical neuron datasets, respectively, revealed that 35% (134 of 380) of upregulated DEGs (minus DEGs from the 1-h time point) in the iDopa dataset were in common with at least one of the other two datasets, highlighting canonical neuronal activity-regulated genes (Table S4). These include *BDNF* and *NTRK2*, consistent with our observation that BDNF/TrkB-signaling contributes to cLTP-mediated potentiation of iDopa neuronal networks.

246 DEGs were upregulated in the cLTP-induced iDopa cultures but not the hiPSC or mouse cortical cultures (Figure 6E; Table S4). GO analyses of these 246 DEGs revealed that multiple significant associations with terms relevant to neural plasticity were still present when compared with GO analyses of the original 407 DEG dataset (Figure 6D). These included, for biological process, "synaptic signaling" and for cellular components, "synapse," suggesting that cLTP induces a distinctive set of genes expressed at the synapse either associated with the specific composition of iDopa cultures or induction paradigm. Of the 46 cLTP-induced genes associated with the GO cellular component term "synapse" (Table S3), 23.9% (11 of 46) have been identified in a recent study (Hu et al., 2018) as loci associated with the neurological disorders schizophrenia (*CHGB*, *GRIN2A*, *IL10RA*, *LDLRAD4*, *SFRP1*, *SLC18A1*, and *TIMP3*) and nicotine addiction (*CACNB2*, *CHRNA6*, *ELM O 1*, *GRIN2A*, and *PDE4D*), notable in light of associations of

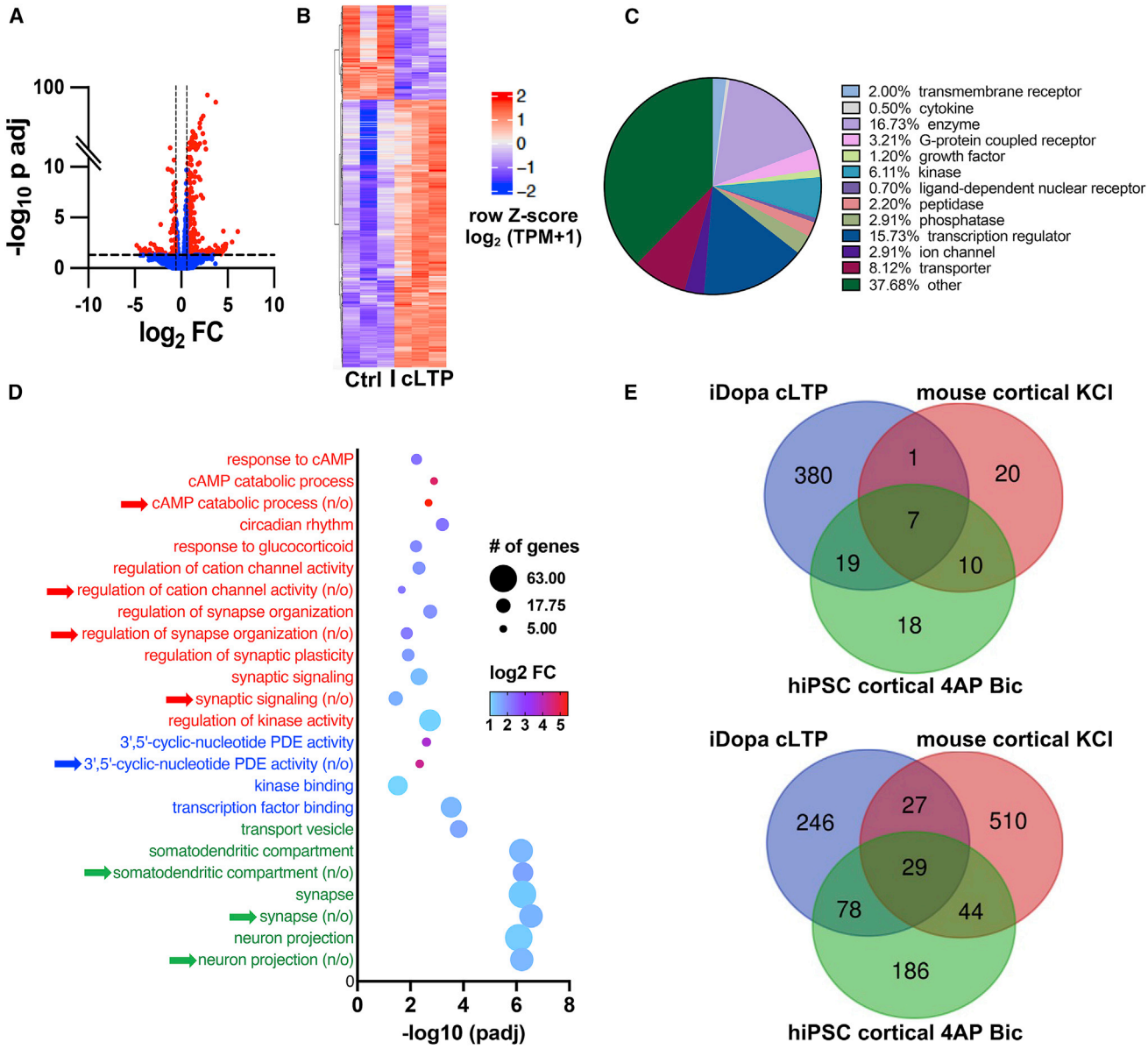

Figure 6. Analysis of cLTP-induced gene expression changes on iDopa neuronal networks 5 h after FSK/ROL washout

(A) Volcano plot showing DEGs comparing cLTP and CTRL (DMSO)-treated co-cultures. Three replicates for each condition were averaged before comparison. Red dots represent genes with a fold change (FC) of 2 or greater and Benjamini-Hochberg adjusted p-value (BH Padj) of 0.05 or less.

(B) Heatmap of significant DEGs (BH Padj $\leq$ 0.05) comparing cLTP and CTRL (DMSO)-treated cultures. Three replicates for each condition are shown, with values as row *Z* scores per gene of Log2(TPM+1)-transformed value (TPM: transcript per million).

(C) Pie chart illustrating classification of the 407 genes significantly upregulated by cLTP.

(D) Dot plot of selected enriched GO terms for biological processes (red), molecular functions (green), and cellular components (blue) for upregulated DEGs when comparing cLTP- and CTRL -treated iDopa cultures. Dot size indicates the number of genes that change, and color indicates FC in the number of cLTP upregulated DEGs over the number of expected genes. The significance of association with the GO term is shown on the x axis. Terms without arrows are from analyses of all 407 DEGs significantly upregulated by cLTP. Terms with arrows are from an analysis of the 246-gene subset of cLTP upregulated DE-Gs that do not overlap with mouse and human iPSC cortical neuron datasets described in (E).

(E) Venn diagrams comparing overlap of significantly upregulated genes from cLTP-treated iDopa cultures with those from KCl-treated mouse primary cortical neurons at 1 h (top) and 6 h (bottom) (Spiegel et al., 2014) and 4AP- and BIC-treated hiPSC-derived cortical neurons at 1 h (top) and 4 h (bottom) (Pruunsild et al., 2017).

See also Tables S2, S3, and S4.

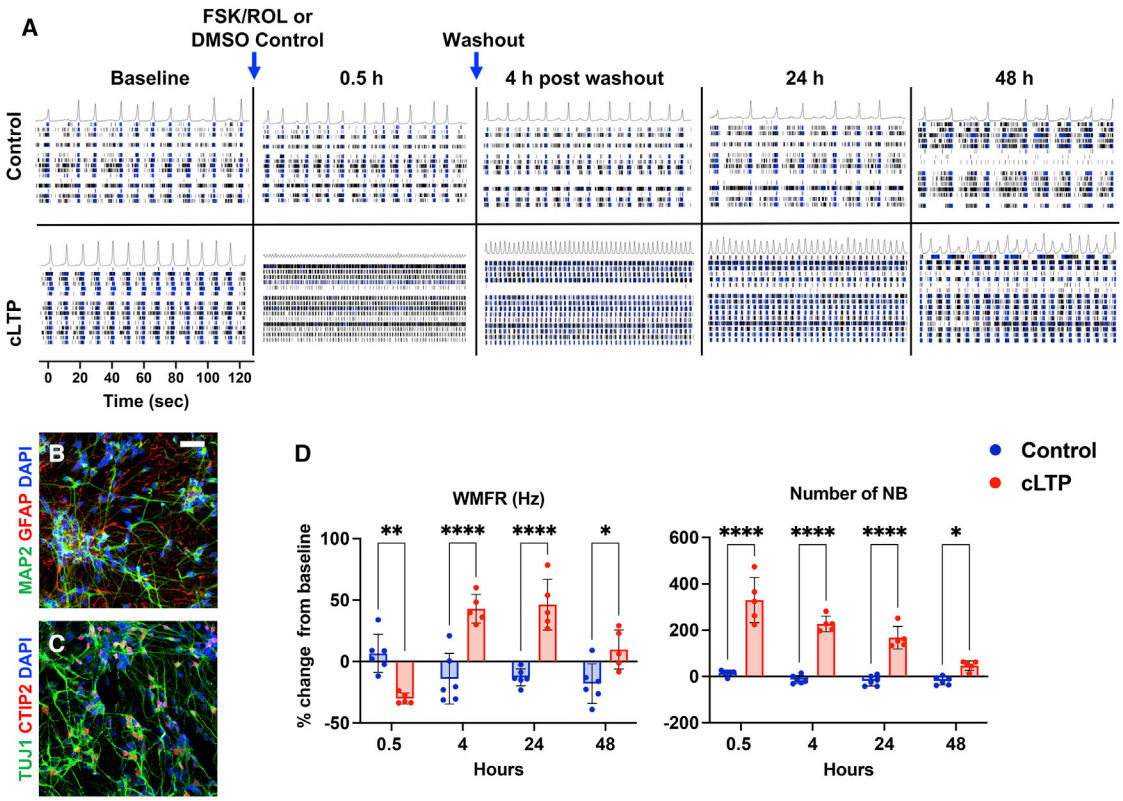

Figure 7. FSK/ROL treatment of hiPSC-derived cortical neuronal networks potentiates activity that persists after drug washout

(A) Raster plots from recordings at baseline, at 30 min (while drugs are still present in the medium), and at the indicated times after FSK/ROL washout.

(B and C) Immunostaining of hiPSC-derived cortical neurons showing Tuj1-positive neurons (green), many of which are co-positive for the layer V/VI cortical neuron marker CTIP2 (red in B). Glial fibrillary acidic protein (GFAP)-positive astrocytes (red in C) are also present in the culture. DAPI is shown in blue. Scale bar in (A), 50 μm for both images.

(D) Analysis of WMFR and number of NB parameters for the experiment shown in (A).

n = 5–6 wells per treatment group. two-way ANOVA, Sidak's multiple comparisons test. Data are shown as mean ± SD, and p values are indicated as *0.05 > p ≥ 0.01; **0.01 > p ≥ 0.001; ***0.001 > p ≥ 0.0001; ****p < 0.0001. The experiment is representative of two independent experiments.

these disorders with the VTA (Chen et al., 2021). Significant associations with terms related to the FSK/ROL paradigm, such as "cAMP catabolic process," were also found (Figure 6D; Table S3). These results demonstrate the potential of using hiPSCs to study mechanisms that underlie activity-regulated gene expression and neural plasticity.

cLTP induces long-lasting potentiation of hiPSC-derived cortical neuronal network activity

LTP has been observed across numerous regions of the mammalian CNS (Kim and Linden, 2007). After demonstrating chemical induction of phenotypes consistent with LTP on iDopa cultures, we next applied the assay to hiPSC-derived cortical neurons we produced. After 4 weeks of differentiation from the neural progenitor cell stage, the culture is comprised primarily of neurons, many of which are positive for the layer V/VI marker CTIP2, with smaller contributions of astrocytes (Figures 7B and 7C). Cells were then plated on MEAs in co-culture with primary human astrocytes (PHAs). We observed that, as for iDopa/iAstro co-cultures, cortical/PHA co-cultures treated with FSK/ROL exhibited persistently increased WMFR and NB frequency after drug washout (Figures 7A and 7D), suggesting that the cLTP assay can be extended to the study of LTP in hiPSC-derived neurons from different brain regions.

DISCUSSION

We describe the development of an MEA-based platform using chemical induction to model LTP on hiPSC-derived neuronal networks. This label-free, non-destructive approach enables tracking of L-LTP for days after

induction. Its 48-well format is amenable to higher-throughput analyses.

FSK/ROL treatment is a well-established cLTP paradigm. Our contention that the responses of iDopa neuronal networks to FSK/ROL treatment reflect an LTP-like phenotype is based on functional and molecular lines of evidence. First, a 30-min exposure potentiates firing and network bursting rates acutely and then for 48–72 h after drug washout, consistent with E-LTP and the long-lasting synaptic strengthening that characterizes L-LTP, respectively. Second, we observed molecular hallmarks of LTP after drug washout, including phosphorylation of CREB, increased IEG protein expression, and a transcriptomic profile at 5 h that is consistent with neuronal activity-regulated expression.

Synaptic plasticity is a fundamental aspect of mature neuronal function that has not been extensively explored in hiPSC-derived neurons. Our cLTP platform complements published studies demonstrating locally induced LTP on networks of hiPSC-derived neurons (Autar et al., 2022; Caneus et al., 2020; Dong et al., 2020; Odawara et al., 2016). These studies support our observation of LTP-like plasticity across cultured hiPSC-derived neuronal networks and underscore the utility of developing multiple complementary approaches. In contrast to cLTP, these local modes of LTP induction offer more physiologically relevant stimulation paradigms. However, the cLTP assay we developed has several advantages, including potentiation that persists for days, allowing longer-term studies of L-LTP, enabling detection of molecular changes by potentiation of the entire network, and, finally, a higher-throughput format.

Our analyses showed that the iDopa cell population we used is a combination of DA, glutamatergic, and GABAergic neurons, with a gene expression signature consistent with ventral midbrain DA nuclei, including the VTA, which is known to be associated with neuropsychiatric and neurodegenerative diseases as well as addictive behaviors (Chen et al., 2021; Langlois and Nugent, 2017). Taken together with our observation that a subset of cLTP-induced upregulated genes associated with the GO term "synapse" have been identified as loci associated with nicotine addiction and schizophrenia (Hu et al., 2018), these data suggest that a cLTP-MEA assay could be a valuable tool to investigate synaptic plasticity in VTA neurons derived from hiPSCs from individuals harboring risk alleles for these disorders. A recent study of hiPSC-derived ventral midbrain DA neurons bearing 16p11.2 copy number variants (CNVs) associated with schizophrenia, autism, and intellectual disability demonstrated hyperactivity on MEAs (Sundberg et al., 2021).

Our study also began to probe the mechanism underlying cLTP on iDopa cultures. In contrast to studies of FSK/ROL-mediated cLTP on mouse hippocampal slices (Otmakhov et al., 2004) and hiPSC-derived cortical neurons (Fink et al., 2021), demonstrating NMDAR dependence, we found that cLTP on iDopa neuronal networks was largely NMDAR independent, with APV only causing a minor reduction in NB frequency 4 h after FSK/ROL washout, but not at 24 h. We also observed that cLTP on iDopa neuronal networks did not depend on several other calcium sources, CP-AMPAR, and L-, R-, and T-type VGCCs. It is possible that there are multiple sources of calcium entry so that blocking only one is not sufficient. There are other potential sources of calcium entry that we did not assess, including N- and P/Q-type VGCCs, metabotropic glutamate receptors, and internal stores, which will be explored in follow-up studies. It is also possible that calcium entry is not required. For instance, in a presynaptic form of LTP that occurs at fibers parallel to Purkinje synapses, elevation of presynaptic cAMP levels via FSK enhances glutamate release even in the presence of the R-type-VGCC blockers, bypassing the calcium trigger that stimulates adenylyl cyclase in this system (Myoga and Regehr, 2011). Finally, the immaturity of iPSC neurons may affect requirements for calcium entry because it has been shown in rodents that signaling cascades that mediate LTP display developmental stage-dependent differences (Lohmann and Kessels, 2014). For instance, rodent studies on rodent hippocampal slices have shown that, in contrast to LTP at mature stages, LTP at neonatal stages requires PKA but not CaMKII (Yasuda et al., 2003).

We also investigated the role of BDNF in FSK/ROL-mediated cLTP on iDopa cultures. We found that BDNF was released into CM collected 1 h after FSK/ROL washout, consistent with reports that TrkB is rapidly activated by FSK-mediated potentiation (Patterson et al., 2001). We showed that cLTP on iDopa neuronal networks partially depends on BDNF, based on our observation that potentiation was attenuated by adding the BDNF scavenger TrkB-Fc. BDNF is a key factor in multiple neurological disorders (Johnstone and Mobley, 2020). Reduced BDNF concentrations have been found in the blood and brain of individuals with psychiatric and neurodegenerative disorders (Lima Giacobbo et al., 2019), and its genetic variants have been implicated in neuropsychiatric and substance dependence disorders (Zhang et al., 2006). Given the critical role of BDNF in plasticity and neurological disease, our observations suggest that FSK/ROL-mediated cLTP will be a valuable assay for studying BDNF activity in hiPSC-based neuronal network models.

Our observation that BDNF was not sufficient to mimic the effects of cLTP-CM suggests that other factors released into the medium 1 h after drug washout are necessary to support cLTP-mediated potentiation. Further analysis of cLTP-CM will be performed in future studies; however, an

obvious candidate is glutamate, consistent with multiple reports of FSK-mediated enhancement of glutamate release (Chavez-Noriega and Stevens, 1994; Kaneko and Takahashi, 2004; Sakaba and Neher, 2001). cLTP-CM potentiated activity when added to CTRL wells, but this potentiation did not reach the same levels, nor did it last as long as that observed when cLTP-CM was added to cLTP-treated wells. Our observation that cLTP-CM elicited short-lasting potentiation on CTRL wells that did not persist after washout suggests that excitatory factors released into the medium are not able to trigger an L-LTP like phenotype on their own and that the initial, early phase FSK/ROL-mediated elevation of cAMP is necessary for this late phase to occur. Our results are consistent with a model where long-lasting FSK/ROL-mediated potentiation of iDopa neuronal networks depends on release of factors, including BDNF, and increased activity-dependent gene expression through activation of CREB.

The cLTP platform we developed offers the opportunity to couple analyses of electrophysiological activity to studies of molecular mechanisms of LTP in hiPSC neuronal networks, a powerful approach in the context of human genetics reflected by hiPSC-based models of neurological disease. The higher-throughput format enables its use for drug screening, optimization of culture conditions that support neuronal plasticity, and phenotype discovery across panels of lines from affected individuals.

EXPERIMENTAL PROCEDURES

Co-culture of iDopa neurons and iCell astrocytes on MEA plates

All human stem cell culture was performed under approval from the Stem Cell Research Oversight (SCRO) panel at Sanford Burnham Prebys Medical Discovery Institute. 48-well MEA plates (Axion BioSystems) were coated following the manufacturer's instructions. iCell DopaNeurons (iDopas) and iCell Astrocytes (iAstros) (Fujifilm Cellular Dynamics) were thawed following the manufacturer's recommendations and resuspended at a ratio of 8:1 in NBA-K medium (Neurobasal A medium (Gibco|Thermo-Fisher Scientific) with 10% Knock-out serum replacement (KOSR) (Gibco|Thermo-Fisher Scientific). See supplemental experimental procedures for complete medium formulation). A 10-μL drop of 80,000 iDopa neurons and 10,000 iAstros was then dispensed directly into the 10 μL drop of laminin in each well. After 45 min in a tissue culture incubator, 300 μL of NBA-K medium was added to each well. Cultures were fed every other day by exchanging 66% of the medium. The culture was maintained in NBA-K medium for the first 5 days after plating. At that point, it was switched to BrainPhys Complete (Bardy et al., 2015). All medium formulations and methods for generation and culture of hiPSC-derived cortical neurons, immunocytochemistry, and image analysis are detailed in the supplemental experimental procedures.

Drug treatments

Drug treatments were performed approximately 4–5 weeks after plating. BrainPhys supplements were removed from the culture medium before drug treatment. For induction of cLTP, an initial baseline recording was taken, and immediately thereafter, 30 μL of medium per well (of a total of 300 μL) was removed. Then 30 μL of medium with a 10× concentration of cLTP drugs was added, and the plate was returned to the incubator. MEA plates were recorded for 5 min at 30 min after drug addition, and then drugs were washed out. The plates were then recorded at the times noted. Drugs used, drug treatment protocols, MEA recording, and MEA data analysis methods are detailed in the supplemental experimental procedures.

RNA-seq analysis

cLTP and DMSO treated iDopa/iAstro co-cultures on 48 well MEA plates were harvested 5 h after FSK/ROL washout. Triplicate samples were prepared for cLTP and CTRL, with each sample comprised of 8 wells combined. Total RNA was isolated using an RNeasy mini kit (QIAGEN) and treated with DNase (QIAGEN). Invitrogen Qubit and Agilent Technologies TapeStation were used to determine RNA concentration and integrity, respectively, before library preparation. Poly(A) RNA was isolated using the NEBNext Poly(A) mRNA Magnetic Isolation Module, and barcoded libraries were made using the NEBNext Ultra II Directional RNA Library Prep Kit for Illumina (New England Biolabs). Libraries were pooled and single end sequenced (1 × 75) on the Illumina NextSeq 500 using the High Output V2 kit (Illumina). RNA-seq data analysis methods are detailed in the supplemental experimental procedures.

Statistical analysis

All statistical tests and sample sizes are included in the figure legends and text. Data in graphs are shown as mean ± SD, and p values are indicated as $*0.05 > p \geq 0.01$, $**0.01 > p \geq 0.001$, $***0.001 > p \geq 0.0001$, $****p < 0.0001$.

Data and code availability

The accession number for the RNA-seq data reported in this paper is Gene Expression Omnibus: GSE193191.

SUPPLEMENTAL INFORMATION

Supplemental information can be found online at https://doi.org/10.1016/j.stemcr.2022.07.012.

AUTHOR CONTRIBUTIONS

D.P., P.K., S.P.S., and H.Z. performed experiments. D.P., A.T.W., and A.G.B. performed data analyses. S.B. and S.H. contributed to assay development. D.P. and A.G.B. designed the experiments. D.P. and A.G.B. wrote the manuscript with input from all authors. A.G.B. and J.G. acquired funding. A.G.B. conceived and guided the project.

ACKNOWLEDGMENTS

We thank Dr. Isabel Onofre for contributions to immunofluorescence studies. We thank Drs. Juan Pina Crespo and Dr. Bruce Aronow for advice. We thank Drs. Brian James, Andrew Hodges, Jun

Yin, and Rabi Murad at the Sanford Burnham Prebys Genomics and Bioinformatics Cores. We thank Dr. Michael Jackson and members of the Prebys Center for support. This work was supported by grants to A.G.B. from the United States Department of Defense, US Air Force (FA8650-18-2-6971), National Institutes of Health (U19MH106434), Janssen Pharmaceuticals, and the Viterbi Family Foundation of the Jewish Community Foundation San Diego, United States.

CONFLICTS OF INTEREST

The authors declare no competing interests.

Received: January 19, 2022
Revised: July 18, 2022
Accepted: July 19, 2022
Published: August 18, 2022

REFERENCES

Alkadhi, K.A. (2021). NMDA receptor-independent LTP in mammalian nervous system. Prog. Neurobiol. *200*, 101986.

Arango-Lievano, M., Borie, A.M., Dromard, Y., Murat, M., Desarmenien, M.G., Garabedian, M.J., and Jeanneteau, F. (2019). Persistence of learning-induced synapses depends on neurotrophic priming of glucocorticoid receptors. Proc. Natl. Acad. Sci. USA *116*, 13097–13106.

Arnold, F.J.L., Hofmann, F., Bengtson, C.P., Wittmann, M., Vanhoutte, P., and Bading, H. (2005). Microelectrode array recordings of cultured hippocampal networks reveal a simple model for transcription and protein synthesis-dependent plasticity. J. Physiol. *564*, 3–19.

Asgrimsdottir, E.S., and Arenas, E. (2020). Midbrain dopaminergic neuron development at the single cell level: in vivo and in stem cells. Front. Cell Dev. Biol. *8*, 463.

Autar, K., Guo, X., Rumsey, J.W., Long, C.J., Akanda, N., Jackson, M., Narasimhan, N.S., Caneus, J., Morgan, D., and Hickman, J.J. (2022). A functional hiPSC-cortical neuron differentiation and maturation model and its application to neurological disorders. Stem Cell Rep. *17*, 96–109.

Baltaci, S.B., Mogulkoc, R., and Baltaci, A.K. (2019). Molecular mechanisms of early and late LTP. Neurochem. Res. *44*, 281–296.

Bardy, C., van den Hurk, M., Eames, T., Marchand, C., Hernandez, R.V., Kellogg, M., Gorris, M., Galet, B., Palomares, V., Brown, J., et al. (2015). Neuronal medium that supports basic synaptic functions and activity of human neurons in vitro. Proc. Natl. Acad. Sci. USA *112*, E2725–E2734.

Bliim, N., Leshchyns'ka, I., Sytnyk, V., and Janitz, M. (2016). Transcriptional regulation of long-term potentiation. Neurogenetics *17*, 201–210.

Bliss, T.V., and Lomo, T. (1973). Long-lasting potentiation of synaptic transmission in the dentate area of the anaesthetized rabbit following stimulation of the perforant path. J. Physiol. *232*, 331–356.

Bolsius, Y.G., Zurbriggen, M.D., Kim, J.K., Kas, M.J., Meerlo, P., Aton, S.J., and Havekes, R. (2021). The role of clock genes in sleep, stress and memory. Biochem. Pharmacol. *191*, 114493.

Bourtchuladze, R., Frenguelli, B., Blendy, J., Cioffi, D., Schutz, G., and Silva, A.J. (1994). Deficient long-term memory in mice with a targeted mutation of the cAMP-responsive element-binding protein. Cell *79*, 59–68.

Brofiga, M., Pisano, M., Raiteri, R., and Massobrio, P. (2021). On the road to the brain-on-a-chip: a review on strategies, methods, and applications. J. Neural. Eng. *18*, 041005.

Caneus, J., Akanda, N., Rumsey, J.W., Guo, X., Jackson, M., Long, C.J., Sommerhage, F., Georgieva, S., Kanaan, N.M., Morgan, D., et al. (2020). A human induced pluripotent stem cell-derived cortical neuron human-on-a chip system to study Abeta42 and tau-induced pathophysiological effects on long-term potentiation. Alzheimers Dement. *6*, e12029.

Castillo, P.E. (2012). Presynaptic LTP and LTD of excitatory and inhibitory synapses. Cold Spring Harb. Perspect. Biol. *4*, a005728.

Chavez-Noriega, L.E., and Stevens, C.F. (1994). Increased transmitter release at excitatory synapses produced by direct activation of adenylate cyclase in rat hippocampal slices. J. Neurosci. *14*, 310–317.

Chen, A.P.F., Chen, L., Kim, T.A., and Xiong, Q. (2021). Integrating the roles of midbrain dopamine circuits in behavior and neuropsychiatric disease. Biomedicines *9*, 647.

Cohen, D., and Segal, M. (2011). Network bursts in hippocampal microcultures are terminated by exhaustion of vesicle pools. J. Neurophysiol. *106*, 2314–2321.

Davis, S., Bozon, B., and Laroche, S. (2003). How necessary is the activation of the immediate early gene zif268 in synaptic plasticity and learning? Behav. Brain Res. *142*, 17–30.

Dong, Y., Xiong, M., Chen, Y., Tao, Y., Li, X., Bhattacharyya, A., and Zhang, S.C. (2020). Plasticity of synaptic transmission in human stem cell-derived neural networks. iScience *23*, 100829.

Fink, J.J., Schreiner, J.D., Bloom, J.E., James, J., Baker, D.S., Robinson, T.M., Lieberman, R., Loew, L.M., Chamberlain, S.J., and Levine, E.S. (2021). Hyperexcitable phenotypes in induced pluripotent stem cell-derived neurons from patients with 15q11-q13 duplication syndrome, a genetic form of autism. Biol. Psychiatry *90*, 756–765.

Gray, J.M., and Spiegel, I. (2019). Cell-type-specific programs for activity-regulated gene expression. Curr. Opin. Neurobiol. *56*, 33–39.

Hardingham, G.E., Pruunsild, P., Greenberg, M.E., and Bading, H. (2018). Lineage divergence of activity-driven transcription and evolution of cognitive ability. Nat. Rev. Neurosci. *19*, 9–15.

Hasselmann, J., and Blurton-Jones, M. (2020). Human iPSC-derived microglia: a growing toolset to study the brain's innate immune cells. Glia *68*, 721–739.

Heikkila, T.J., Ylä-Outinen, L., Tanskanen, J.M.A., Lappalainen, R.S., Skottman, H., Suuronen, R., Mikkonen, J.E., Hyttinen, J.A.K., and Narkilahti, S. (2009). Human embryonic stem cell-derived neuronal cells form spontaneously active neuronal networks in vitro. Exp. Neurol. *218*, 109–116.

Hu, Y., Fang, Z., Yang, Y., Rohlsen-Neal, D., Cheng, F., and Wang, J. (2018). Analyzing the genes related to nicotine addiction or schizophrenia via a pathway and network based approach. Sci. Rep. *8*, 2894.

Huang, Y.Y., and Kandel, E.R. (1998). Postsynaptic induction and PKA-dependent expression of LTP in the lateral amygdala. Neuron *21*, 169–178.

Johnstone, A., and Mobley, W. (2020). Local TrkB signaling: themes in development and neural plasticity. Cell Tissue Res. *382*, 101–111.

Jung, N.H., Janzarik, W.G., Delvendahl, I., Münchau, A., Biscaldi, M., Mainberger, F., Bäumer, T., Rauh, R., and Mall, V. (2013). Impaired induction of long-term potentiation-like plasticity in patients with high-functioning autism and Asperger syndrome. Dev. Med. Child Neurol. *55*, 83–89.

Kaneko, M., and Takahashi, T. (2004). Presynaptic mechanism underlying cAMP-dependent synaptic potentiation. J. Neurosci. *24*, 5202–5208.

Kim, H.J., Kim, M., Kang, B., Yun, S., Ryeo, S.E., Hwang, D., and Kim, J.H. (2019). Systematic analysis of expression signatures of neuronal subpopulations in the VTA. Mol. Brain *12*, 110.

Kim, S.J., and Linden, D.J. (2007). Ubiquitous plasticity and memory storage. Neuron *56*, 582–592.

Knapska, E., and Kaczmarek, L. (2004). A gene for neuronal plasticity in the mammalian brain: Zif268/Egr-1/NGFI-A/Krox-24/TIS8/ZENK? Prog. Neurobiol. *74*, 183–211.

Kolb, B. (1984). Functions of the frontal cortex of the rat: a comparative review. Brain Res. *320*, 65–98.

Langlois, L.D., and Nugent, F.S. (2017). Opiates and plasticity in the ventral tegmental area. ACS Chem. Neurosci. *8*, 1830–1838.

Lima Giacobbo, B., Doorduin, J., Klein, H.C., Dierckx, R.A.J.O., Bromberg, E., and de Vries, E.F.J. (2019). Brain-derived neurotrophic factor in brain disorders: focus on neuroinflammation. Mol. Neurobiol. *56*, 3295–3312.

Lohmann, C., and Kessels, H.W. (2014). The developmental stages of synaptic plasticity. J. Physiol. *592*, 13–31.

Lu, K.T., and Gean, P.W. (1999). Masking of forskolin-induced long-term potentiation by adenosine accumulation in area CA1 of the rat hippocampus. Neuroscience *88*, 69–78.

Luscher, C., and Malenka, R.C. (2012). NMDA receptor-dependent long-term potentiation and long-term depression (LTP/LTD). Cold Spring Harb. Perspect. Biol. *4*, a005710.

Mameli, M., and Lüscher, C. (2011). Synaptic plasticity and addiction: learning mechanisms gone awry. Neuropharmacology *61*, 1052–1059.

Mateos-Aparicio, P., and Rodríguez-Moreno, A. (2019). The impact of studying brain plasticity. Front. Cell. Neurosci. *13*, 66.

Molnar, E. (2011). Long-term potentiation in cultured hippocampal neurons. Semin. Cell Dev. Biol. *22*, 506–513.

Mould, A.W., Hall, N.A., Milosevic, I., and Tunbridge, E.M. (2021). Targeting synaptic plasticity in schizophrenia: insights from genomic studies. Trends Mol. Med. *27*, 1022–1032.

Myoga, M.H., and Regehr, W.G. (2011). Calcium microdomains near R-type calcium channels control the induction of presynaptic long-term potentiation at parallel fiber to purkinje cell synapses. J. Neurosci. *31*, 5235–5243.

Nakagawa, M., Koyanagi, M., Tanabe, K., Takahashi, K., Ichisaka, T., Aoi, T., Okita, K., Mochiduki, Y., Takizawa, N., and Yamanaka, S. (2008). Generation of induced pluripotent stem cells without Myc from mouse and human fibroblasts. Nat. Biotechnol. *26*, 101–106.

Nicoll, R.A. (2017). A brief history of long-term potentiation. Neuron *93*, 281–290.

Niedringhaus, M., Chen, X., Dzakpasu, R., and Conant, K. (2012). MMPs and soluble ICAM-5 increase neuronal excitability within in vitro networks of hippocampal neurons. PLoS One *7*, e42631.

Odawara, A., Katoh, H., Matsuda, N., and Suzuki, I. (2016). Induction of long-term potentiation and depression phenomena in human induced pluripotent stem cell-derived cortical neurons. Biochem. Biophys. Res. Commun. *469*, 856–862.

Odawara, A., Saitoh, Y., Alhebshi, A.H., Gotoh, M., and Suzuki, I. (2014). Long-term electrophysiological activity and pharmacological response of a human induced pluripotent stem cell-derived neuron and astrocyte co-culture. Biochem. Biophys. Res. Commun. *443*, 1176–1181.

Opitz, T., De Lima, A.D., and Voigt, T. (2002). Spontaneous development of synchronous oscillatory activity during maturation of cortical networks in vitro. J. Neurophysiol. *88*, 2196–2206.

Otmakhov, N., Khibnik, L., Otmakhova, N., Carpenter, S., Riahi, S., Asrican, B., and Lisman, J. (2004). Forskolin-induced LTP in the CA1 hippocampal region is NMDA receptor dependent. J. Neurophysiol. *91*, 1955–1962.

Padamsey, Z., Foster, W.J., and Emptage, N.J. (2019). Intracellular Ca(2+) release and synaptic plasticity: a tale of many stores. Neuroscientist *25*, 208–226.

Panja, D., and Bramham, C.R. (2014). BDNF mechanisms in late LTP formation: a synthesis and breakdown. Neuropharmacology *76 Pt C*, 664–676.

Park, H., and Poo, M.M. (2013). Neurotrophin regulation of neural circuit development and function. Nat. Rev. Neurosci. *14*, 7–23.

Patterson, S.L., Pittenger, C., Morozov, A., Martin, K.C., Scanlin, H., Drake, C., and Kandel, E.R. (2001). Some forms of cAMP-mediated long-lasting potentiation are associated with release of BDNF and nuclear translocation of phospho-MAP kinase. Neuron *32*, 123–140.

Pegoraro, S., Broccard, F.D., Ruaro, M.E., Bianchini, D., Avossa, D., Pastore, G., Bisson, G., Altafini, C., and Torre, V. (2010). Sequential steps underlying neuronal plasticity induced by a transient exposure to gabazine. J. Cell. Physiol. *222*, 713–728.

Picconi, B., Piccoli, G., and Calabresi, P. (2012). Synaptic dysfunction in Parkinson's disease. Adv. Exp. Med. Biol. *970*, 553–572.

Poulin, J.F., Gaertner, Z., Moreno-Ramos, O.A., and Awatramani, R. (2020). Classification of midbrain dopamine neurons using single-cell gene expression profiling approaches. Trends Neurosci. *43*, 155–169.

Pruunsild, P., Bengtson, C.P., and Bading, H. (2017). Networks of cultured iPSC-derived neurons reveal the human synaptic activity-regulated adaptive gene program. Cell Rep. *18*, 122–135.

Qiu, J., McQueen, J., Bilican, B., Dando, O., Magnani, D., Punovuori, K., Selvaraj, B.T., Livesey, M., Haghi, G., Heron, S., et al. (2016). Evidence for evolutionary divergence of activity-dependent gene expression in developing neurons. Elife *5*, e20337.

Ronchi, S., Buccino, A.P., Prack, G., Kumar, S.S., Schröter, M., Fiscella, M., and Hierlemann, A. (2021). Electrophysiological phenotype characterization of human iPSC-derived neuronal cell lines by means of high-density microelectrode arrays. Adv. Biol. *5*, e2000223.

Sakaba, T., and Neher, E. (2001). Preferential potentiation of fast-releasing synaptic vesicles by cAMP at the calyx of Held. Proc. Natl. Acad. Sci. USA *98*, 331–336.

Selkoe, D.J. (2002). Alzheimer's disease is a synaptic failure. Science *298*, 789–791.

Spiegel, I., Mardinly, A.R., Gabel, H.W., Bazinet, J.E., Couch, C.H., Tzeng, C.P., Harmin, D.A., and Greenberg, M.E. (2014). Npas4 regulates excitatory-inhibitory balance within neural circuits through cell-type-specific gene programs. Cell *157*, 1216–1229.

Sundberg, M., Pinson, H., Smith, R.S., Winden, K.D., Venugopal, P., Tai, D.J.C., Gusella, J.F., Talkowski, M.E., Walsh, C.A., Tegmark, M., et al. (2021). 16p11.2 deletion is associated with hyperactivation of human iPSC-derived dopaminergic neuron networks and is rescued by RHOA inhibition in vitro. Nat. Commun. *12*, 2897.

Takahashi, K., Tanabe, K., Ohnuki, M., Narita, M., Ichisaka, T., Tomoda, K., and Yamanaka, S. (2007). Induction of pluripotent stem cells from adult human fibroblasts by defined factors. Cell *131*, 861–872.

Tao, Y., and Zhang, S.C. (2016). Neural subtype specification from human pluripotent stem cells. Cell Stem Cell *19*, 573–586.

Tiklova, K., Björklund, Å.K., Lahti, L., Fiorenzano, A., Nolbrant, S., Gillberg, L., Volakakis, N., Yokota, C., Hilscher, M.M., Hauling, T., et al. (2019). Single-cell RNA sequencing reveals midbrain dopamine neuron diversity emerging during mouse brain development. Nat. Commun. *10*, 581.

Yasuda, H., Barth, A.L., Stellwagen, D., and Malenka, R.C. (2003). A developmental switch in the signaling cascades for LTP induction. Nat. Neurosci. *6*, 15–16.

Yokoi, R., Okabe, M., Matsuda, N., Odawara, A., Karashima, A., and Suzuki, I. (2019). Impact of sleep-wake-associated neuromodulators and repetitive low-frequency stimulation on human iPSC-derived neurons. Front. Neurosci. *13*, 554.

Zak, N., Moberget, T., Bøen, E., Boye, B., Waage, T.R., Dietrichs, E., Harkestad, N., Malt, U.F., Westlye, L.T., Andreassen, O.A., et al. (2018). Longitudinal and cross-sectional investigations of long-term potentiation-like cortical plasticity in bipolar disorder type II and healthy individuals. Transl. Psychiatry *8*, 103.

Zhang, H., Ozbay, F., Lappalainen, J., Kranzler, H.R., van Dyck, C.H., Charney, D.S., Price, L.H., Southwick, S., Yang, B.Z., Rasmussen, A., et al. (2006). Brain derived neurotrophic factor (BDNF) gene variants and Alzheimer's disease, affective disorders, posttraumatic stress disorder, schizophrenia, and substance dependence. Am. J. Med. Genet. B Neuropsychiatr. Genet. *141B*, 387–393.